Journal of Electronic Materials, Vol. 9, No. 2, 1980

SOME ELECTRICAL AND OPTICAL PROPERTIES OF A-Si:F:H ALLOYS

A. Madan, S.R. Ovshinsky, W. Czubatyj
Energy Conversion Devices, Inc.
Troy, Michigan 48084
and
M. Shur
University of Minnesota
Department of Electrical Engineering
Minneapolis, Minnesota 55455

(Received July 19, 1979)

Amorphous Si:F:H with desirable properties for photovoltaic applications can be fabricated by the glow discharge of SiF_4 and H_2. The preparation conditions influence the properties of the resultant alloy. For instance, altering the ratio of SiF_4 to H_2 from 80 to 5 can alter the localized state density from $10^{19}cm^{-3}eV^{-1}$ to $\simeq 10^{16}cm^{-3}eV^{-1}$, respectively. The conduction mechanisms are altered and there are vast changes in the photoconductivity as the density of recombination centers is decreased. The lower density of states achieved in the a-Si:F:H alloy reflects in the ease of doping. In addition, the lower density of states in a-Si:F:H alloy should result in a wider depletion region than reported for the a-Si:H alloy when fabricated within the device configuration. Results of C-V measurements using Au Schottky barrier devices confirm this.

Key words: Amorphous silicon, photovoltaic material.

Introduction

In earlier papers we had indicated that amorphous

0361-5235/80/0300-0385$03.00/1 © 1980 AIME

silicon containing fluorine and hydrogen (1-4) possess desirable properties for photovoltaic applications. Amorphous elemental demiconductors ordinarily possess a very large density of localized states which act as shallow traps leading to low values for the drift mobility and deep traps which lead to low recombination lifetimes of free carriers. However, Spear and his group (5,6) reported that amorphous silicon decomposed from silane gas by radio frequency glow discharge and deposited on a heated substrate produces a film which has a very low density of states. However, materials prepared in this way possess a large concentration of hydrogen. Because of the low density of states, these types of films can be doped p-type or n-type (7). Furthermore, the material has a sufficiently high carrier lifetime that efficiencies exceeding 5% have been reported (8). In this paper we detail some of the properties of amorphous Si:F:H alloy. We show that the density of states is lower than in amorphous Si:H material and that it can be doped more easily. The consequence of this is that the depletion width in the devices is wider, which is crucial for obtaining high efficiency devices.

Experimental Details

The radio frequency glow discharge apparatus used was the capacitive kind described by Knights (9). All components of the reaction chamber and gas handling system were constructed of stainless steel. The system was pumped to a pressure of less than 20mTorr prior to deposition. The premixed SiF_4 (Matheson, purity 99.50%) and H_2 gases were fed into the system at a constant rate, and the pressure was maintained at ~ 1 Torr during deposition. The plasma was generated between plates using a radio frequency discharge operating at 13.56 MHz.

The samples were deposited on a heated Corning

7059 glass substrates. In the remainder of the paper, we refer to a nominal substrate temperature, T_s, although the actual substrate temperature is somewhat lower. This is because the observation of T_s was made with a thermocouple somewhat removed from contact with the substrate. The actual substrate temperature is measured to be lower by about 120°C for $T_s >$ 250°C in the absence of a plasma. However, we expect a slight increase in the substrate temperature in the presence of a plasma. The typical deposition rates were 10Å/s.

The samples were furnished with evaporated Al contacts in a coplanar configuration with a 1mm electrode spacing. Linear I-V characteristics for electric fields up to 10^4 V cm^{-1} were generally observed.

The dark conductivity (σ_D) as a function of temperature on the samples was measured in a vacuum better than 10^{-5}Torr; optical absorption was measured using a Beckmann DU spectrophotometer over the spectral range 400-1200nm using a slit width 0.1mm.

In the field-effect experiment, (5,6) the gate voltage was applied across a borosilicate (100μ m thick) glass disc or a quartz substrate (380 μm thick). This experiment was conducted in a vacuum to minimize arcing when a large gate voltage (V_F) was applied. The source to drain current, i, through the sample was measured as a function of the gate voltage, V_F, using a Keithley Electrometer. The analysis used in deriving the density of states, g (E), from i (V_F) curves has been detailed elsewhere (5,6). Since the effect due to the surface states has been neglected, the numbers for the localized state density represent an upper limit.

In this section we shall discuss the properties of the amorphous films as a function of the premix gas ratio SiF_4/H_2 = r. These films exhibit reproducible characteristics, and for a gas ratio r $\simeq$ 10 possess a low density of localized states and exhibit a high photoconductiv-

ity. All the samples were deposited with a nominal radio frequency power of $\simeq$ 50W and at a nominal substrate temperature of $T_s = 380^oC$.

Electrical and Optical Properties

Fig. 1 shows log σ_D vs $10^3/T$ for several samples using gas ratios (r) in the range 10 to 99. As the ratio r is increased, the conduction mechanism changes from a well-defined process to an unactivated process. Samples C and D can be described by the equation,

$$\sigma = \sigma_o \exp\left[-(\Delta E)_T/KT\right]$$

and the pre-exponent $\sigma_o = e\mu_o g(E)kT$, where μ_o is the mobility of the carriers, g(E) the density of states in which they move, and the conductivity activation energy $(\Delta E)_T = \Delta E_O - \delta T$, where δ is assumed to be $\simeq 2 \times 10^{-4} eVK^{-1}$ (10). As will be discussed later, these samples were n type. For C, the pre-exponent $\sigma_o \sim 10^3 (\Omega\ cm)^{-1}$ and since $\mu_o \lesssim 10\ cm^2\ s^{-1}V^{-1}$ yields $N(E_c) > 10^{21}\ cm^{-3}eV^{-1}$. It follows that the dominant conduction mechanism is extended state conduction at the band edge E_c.

As shown in the inset of Fig. 1, samples A and B can be fitted to Mott's (11) formula,

$$\sigma = \sigma_o \exp\left[-\left(\frac{T_o}{T}\right)^{1/4}\right]$$

where $T_o = 2\left[\alpha^3/g(E)k\right]^{1/4}$, and g(E) is the density of localized states, k is the Boltzmann constant, and α is the decay of the electronic wave function. Assuming $\alpha^{-1} \simeq 10Å$ results in an estimate of the density at the Fermi level to be greater than $10^{19}\ cm^{-3}eV^{-1}$. This value is in close agreement with the density of states derived from the field-effect data as will be discussed below.

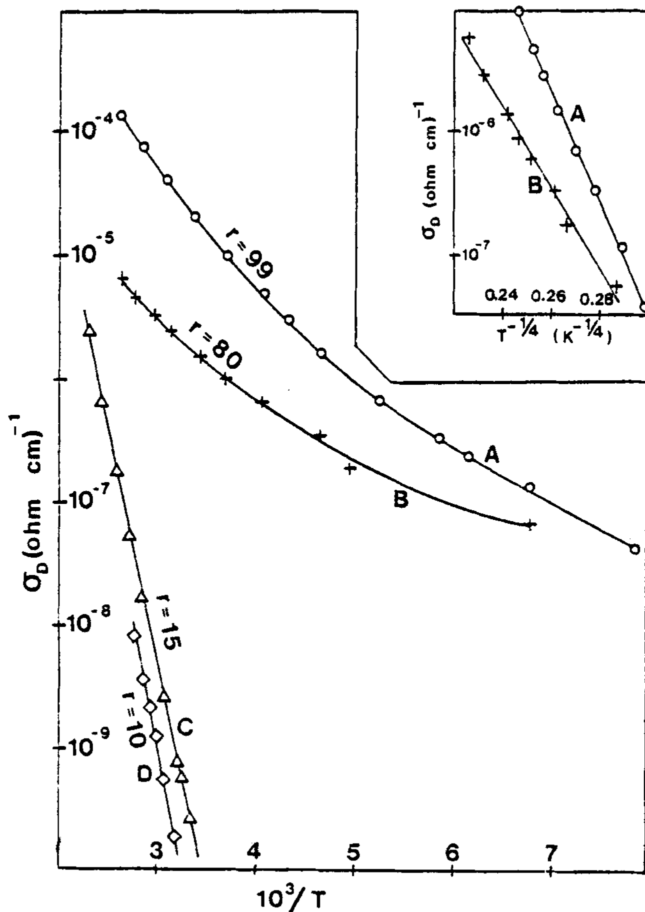

Fig. 1. The dark conductivity, σ_D, is plotted against reciprocal temperature for samples fabricated from different gas ratios, r = SiF_4/H_2. The inset shows σ_D as a function of $T^{-1/4}$ for high values of r.

Fig. 2 summarizes the following parameters: room temperature dark conductivity σ_D $(\Omega cm)^{-1}$, the conduct-

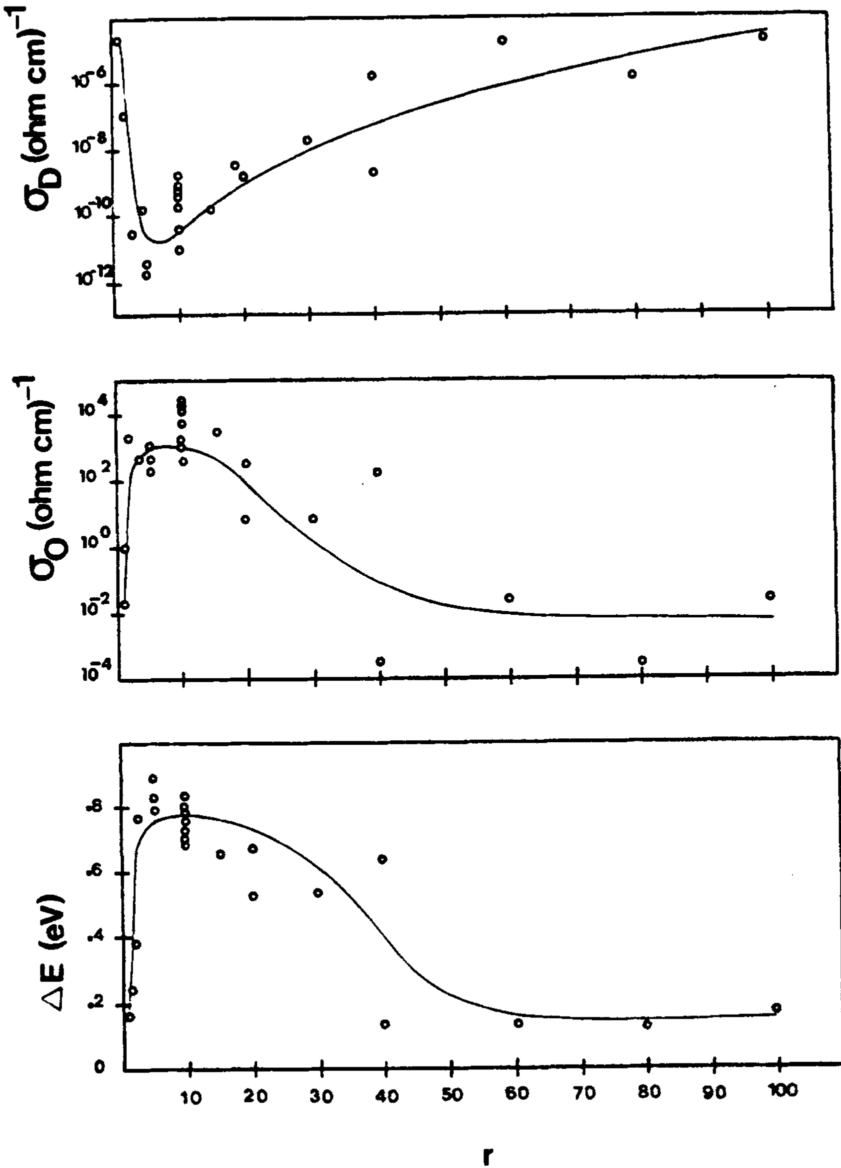

Fig. 2. Parameters σ_D, σ_o and ΔE as defined in the text plotted as a function of gas ratio $r = SiF_4/H_2$.

ivity activation energy ΔE (eV) and the pre-exponent σ_o as a function of r. For samples A and B and similar specimens, a tangent was drawn to the curve of σ_D vs reciprocal temperature at room temperature to obtain an approximate value of ΔE. However, ΔE should not be interpreted as an activation energy in this region. The Figure shows quite clearly that the conduction mechanism changes quite markedly with r, the reason for which is explained below.

Field Effect

The analysis used in deriving the density of states, g(E), from i (V_F) curves neglects the effects of surface states and consequently the numbers for the density of states represent an upper limit. Also, the choice of the flat band position can somewhat alter g(E). We should emphasize that the same procedure has been used for the a-Si:F:H as was used for the a-Si:H alloy (6). As a further check, g(E) was measured for a sample deposited using SiH_4 gas at $T_s = 380^oC$, and power = 10W. The electrical properties were $\sigma_D \sim 10^{-8}\ (\Omega\ cm)^{-1}$ and $\Delta E = 0.60$ eV, and its density of states spectrum was in substantial agreement with the curve obtained by Madan et al. (6) for a sample deposited at a nominal temperature of 570K.

A typical source to drain current (i) as a function of gate voltage (V_F) for a-Si:F:H alloy is shown in the inset of Fig. 3. The arrow indicates the assumed flat band position. For samples fabricated with $5 < r < 99$, n-type response was observed. The experimental g(E) have been crudely extrapolated to the conduction band edge, E_c, whose $g(E) \sim 10^{21}\ cm^{-3}eV^{-1}$, as estimated earlier.

The change in the conduction mechanism with r, as shown in Figs. 1 and 2, becomes understandable in view of the field-effect data. We previously noted that in Fig. 1, as r decreases from 80 to 10, the predominant transport mechanism changes from a variable range hopping-

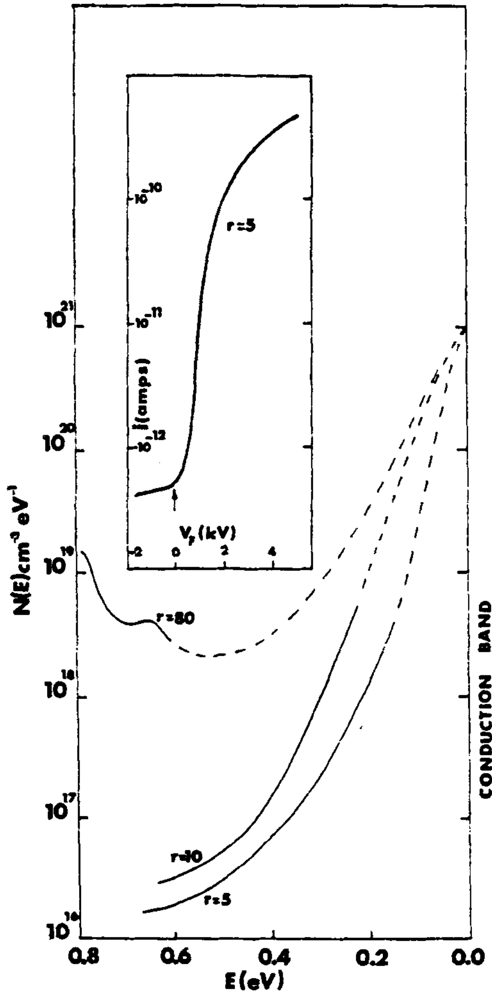

Fig. 3. The localized density of states g(E) ($cm^{-3}eV^{-1}$) plotted for different gas ratios, r = SiF_4/H_2. The inset shows a typical i(V_F) curve and the arrow indicates the assumed flat band positions.

type conduction to a well-defined activated process. As shown above, both samples were n-type and for r = 10, g(E) is orders of magnitude lower than that possessed by r = 80. Since for large values r the density of states is high, the dominant conduction is via localized states in the vicinity of the Fermi level. As r is decreased, as shown in Fig. 3, the density of states decreases sufficiently so that the conduction changes to an activated process.

Fig. 4 shows a more complete density of states spectrum over the energy gap for a-Si:F:H alloy as determined by doping the material n-type and p-type, using P and B as the dopant species. The arrows indicate the extent of the experimental results. Further, the results have been crudely extrapolated to the band edges. For comparison purposes we have also included the density of states spectrum for the a-Si:H alloys which was derived in a similar fashion. We should note that apart from a reduction in g(E) for a-Si:F:H alloys, the peak in g(E) observed for a-Si:H is absent in a-Si:F:H alloys. Further evidence for this lowering in the density of states is provided when we consider the n-type doping characteristics of the two types of materials.

Optical Absorption

Fig. 5 shows the absorption coefficient as a function of wavelength and superimposed is the AM-1 solar spectrum. For comparison purposes, we have included the absorption coefficient for crystalline Si.

Photoconductivity

Amorphous films fabricated from r > 30 did not exhibit any significant photoconductivity. This is not surprising since g(E) is quite large for these types of films, as shown in Fig. 3.

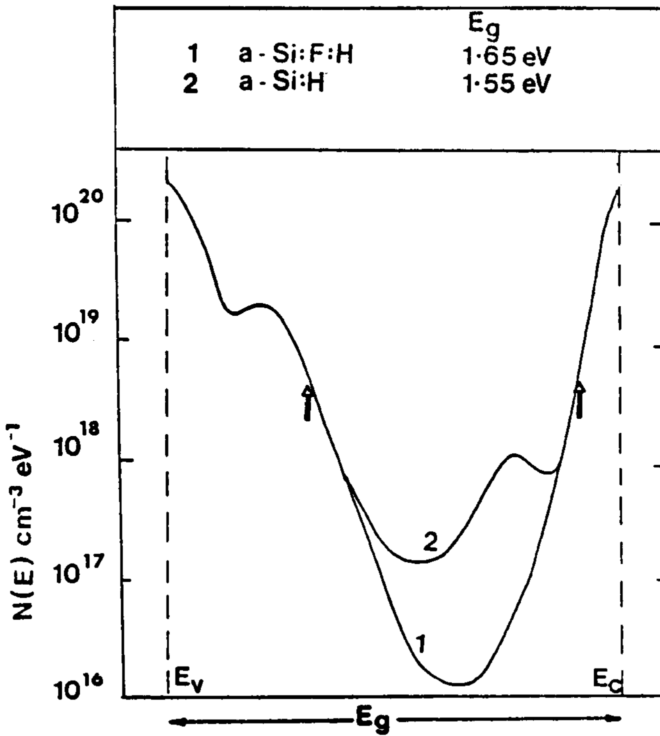

Fig. 4. The variation of the density of states for a-Si:H (6) and a-Si:F:H alloys. The arrows indicate the extent of the experimental data for a-Si:F:H alloy.

With decreasing r the photoconductivity of the samples increases markedly, as shown in Fig. 6. The Figure shows the photoconductivity parameter $\sigma_p = \sigma_L - \sigma_D$, where σ_L is the photoconductivity under illumination for incident illumination at $\lambda = 600$nm with photon flux of $N_o = 10^{15} s^{-1} cm^{-2}$.

Fig. 7 shows the parameter γ as a function of the

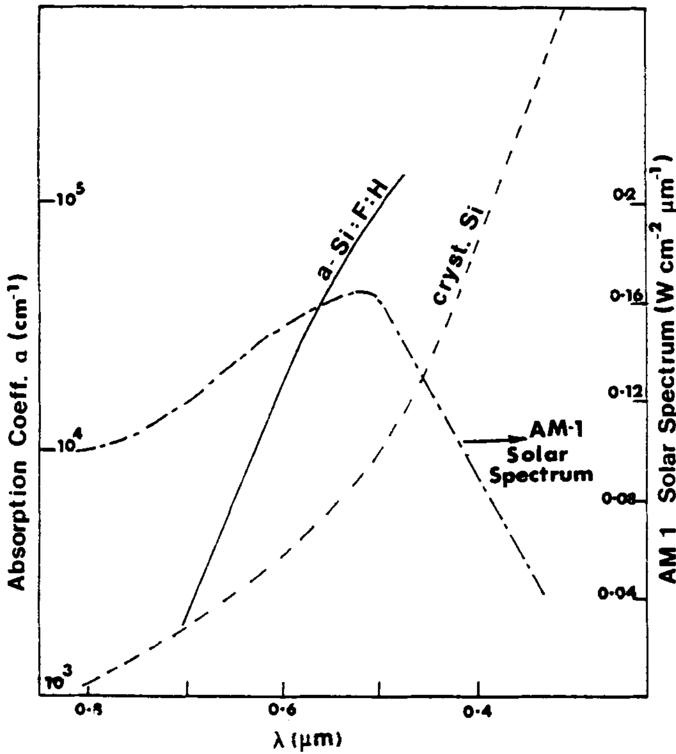

Fig. 5. The absorption coefficient, α , is plotted as a function of wavelength for a-Si:F:H and crystalline Si. Included in the diagram is the AM-1 solar spectrum.

gas ratio r , where γ is defined by $i_p = kF^{\gamma}$, where F is the intensity of the incident radiation and k is a constant. The measurements were made at λ = 600nm and the intensity varied from $10^{12}cm^{-2}s^{-1}$ to $10^{15}cm^{-2}s^{-1}$.

In the above, we note that as the gas ratio r is decreased, the photoconductivity, σ_p , rapidly increases whereas the factor γ remains constant ($\lesssim$ 0.70). Generally, at low level and high level illumination intensities, γ should change from 1.0 to 0.5., respectively. This type of transition could not be distinguished (γ remained constant at $\simeq$ 0.6.) even when we extended the illumina-

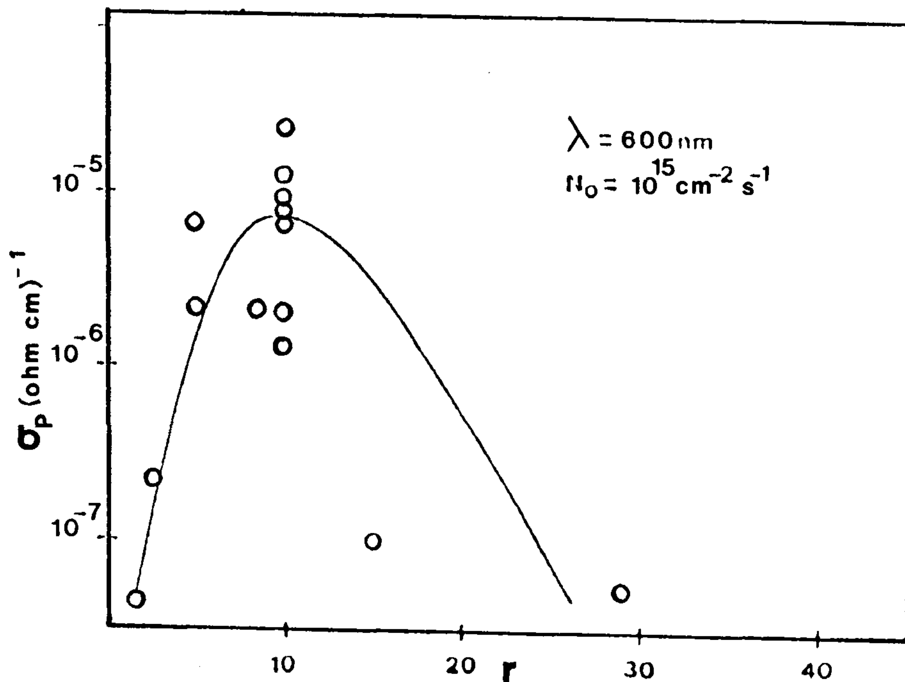

Fig. 6. The photoconductivity, σ_p $(\Omega\, cm)^{-1}$, is plotted as a function of gas ratio $r = SiF_4/H_2$ for incident illumination intensity of 10^{15} cm^{-2} s^{-1} at $\lambda = 600nm$.

tion intensity over a wider range from $N_o = 10^{11}$ s^{-1} cm^{-2} to 5×10^{15} $s^{-1}cm^{-1}$ at $\lambda = 600nm$ for a sample fabricated using fas ratio r = 10. We, therefore, suggest that the predominant recombination does not occur via the deep states around the Fermi energy level. It is possible that the main recombination could occur between trap levels just below the conduction band edge to levels situated just above the valence band edge. As Fig. 6 shows, by changing the gas ratio, and hence the final composition of the alloy, marked changes in σ_p occur, and this could be associated with the change in the above-mentioned trap level densities.

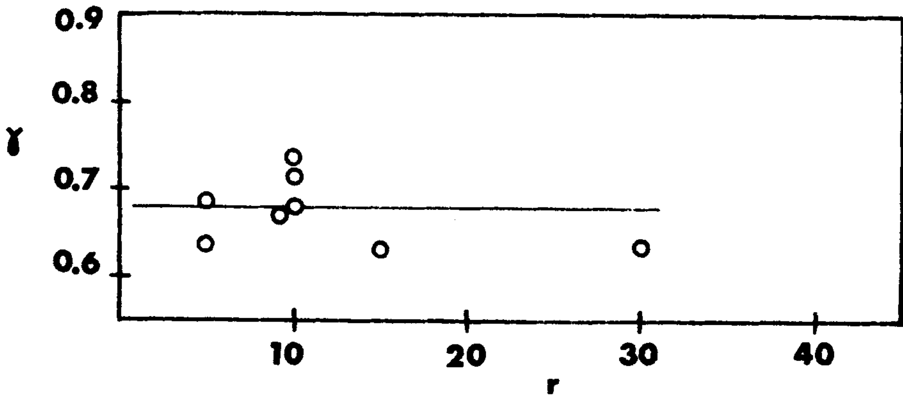

Fig. 7. The constant γ, as defined in the text, is plotted as a function of the gas ratio $r = SiF_4/H_2$.

N-Type Doping

Earlier, we had indicated a reduction in the density of states for the a-Si:F:H, especially in the upper half of the band gap. This reduction reflects in the ease of doping as shown in Fig. 8. The Figure shows the variation of the parameters σ_D and ΔE with the controlled addition of AsH_3 and PH_3 introduced into the premix. We note that very high dark conductivities ($\gtrsim$ 5 $(\Omega\ cm)^{-1}$) with correspondingly low activation energies can be achieved with the addition of very small amounts of dopants. The apparent difference in the two n-type dopant curves shown in Fig. 8 can be explained by recalling that As-H bond is weaker than the P-H bond and hence for a particular power employed, As would therefore be preferentially deposited in relation to P.

These doping characteristics represent a significant improvement over the reported doping characteristics of a-Si:H alloy, (7) as can be clearly seen in Fig. 9, which shows the σ_D and ΔE as a function vppm of PH_3. The improved doping characteristics are a consequence of

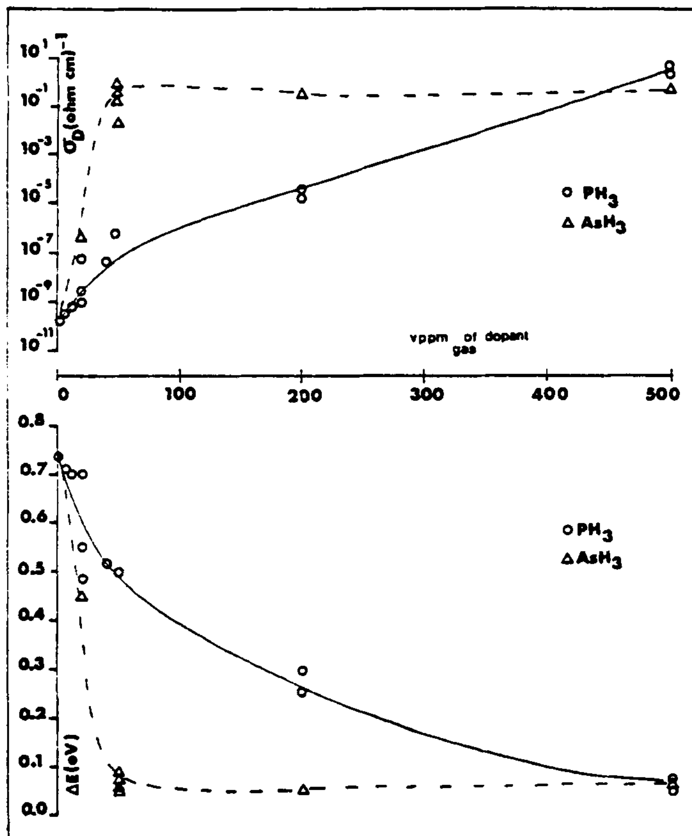

Fig. 8. The room temperature dark conductivity, σ_D $(\Omega\ \mathrm{cm})^{-1}$ and the conductivity activation energy, ΔE (eV) plotted as a function of vppm of PH_3 and AsH_3, which is introduced into the premix gas ratio of $r = SiF_4/H_2 = 10$.

a reduction in the density of states for a-Si:F:H alloy. However, it is also possible that the donor species P/As were utilized more effectively in a-Si:F:H alloy.

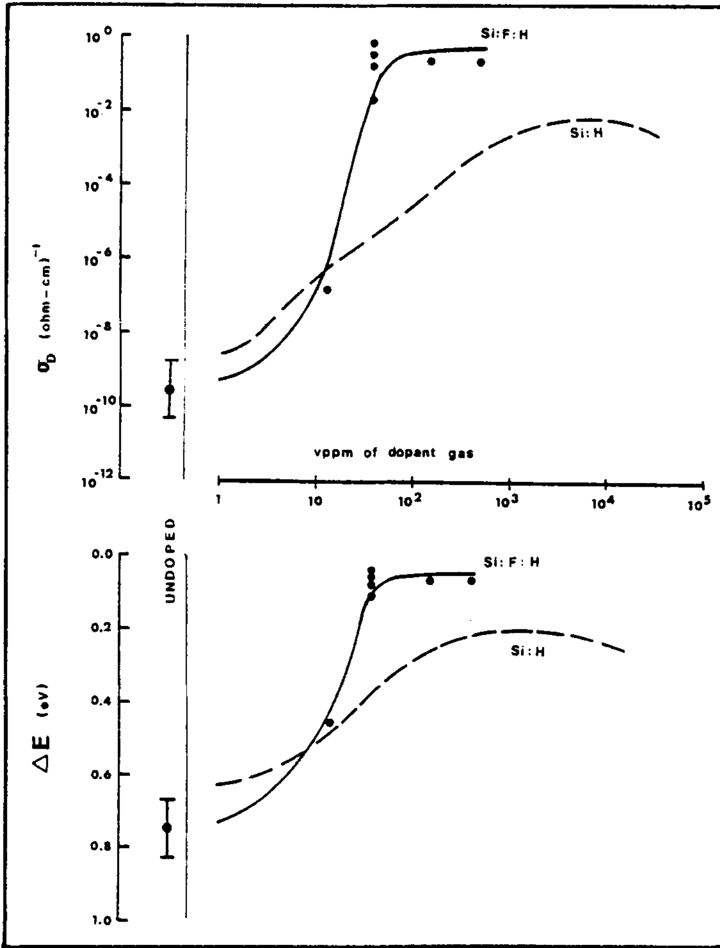

Fig. 9. The comparison of the room temperature dark conductivity, σ_D $(\Omega\,\mathrm{cm})^{-1}$ and activation energy ΔE (eV) is shown for a-Si:H (6) and a-Si:F:H alloy.

C-V Measurements

These types of measurements can provide valuable information about the density of states and the width of the depletion layers. In amorphous materials containing large

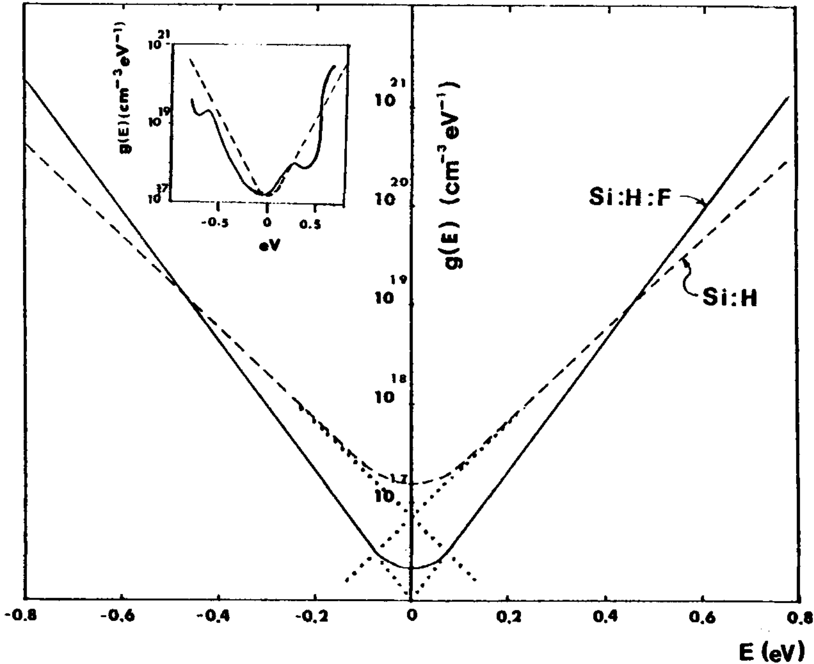

Fig. 10. Analytical approximation, as defined in the text, for the density of states in amorphous silicon-based materials yields the dotted line for a-Si:H material and the solid line for a-Si:F:H material. The inset shows the comparison between the assumed density of states and the measured density of states for a-Si:H alloy (6)

localized state densities, we have to distinguish between two limiting cases: (1) the low frequency region, in which case the space charge density within the depletion layer related to the deep levels has sufficient time to respond to the ac signal variation, and (2) the high frequency region, in which case the space charge distribution is frozen and the response to the applied voltage comes from mobile carriers in the semiconductor at the boundary of the depletion layer.

In order to interpret, we present a very simple model for the density of states (12). We assume that the density

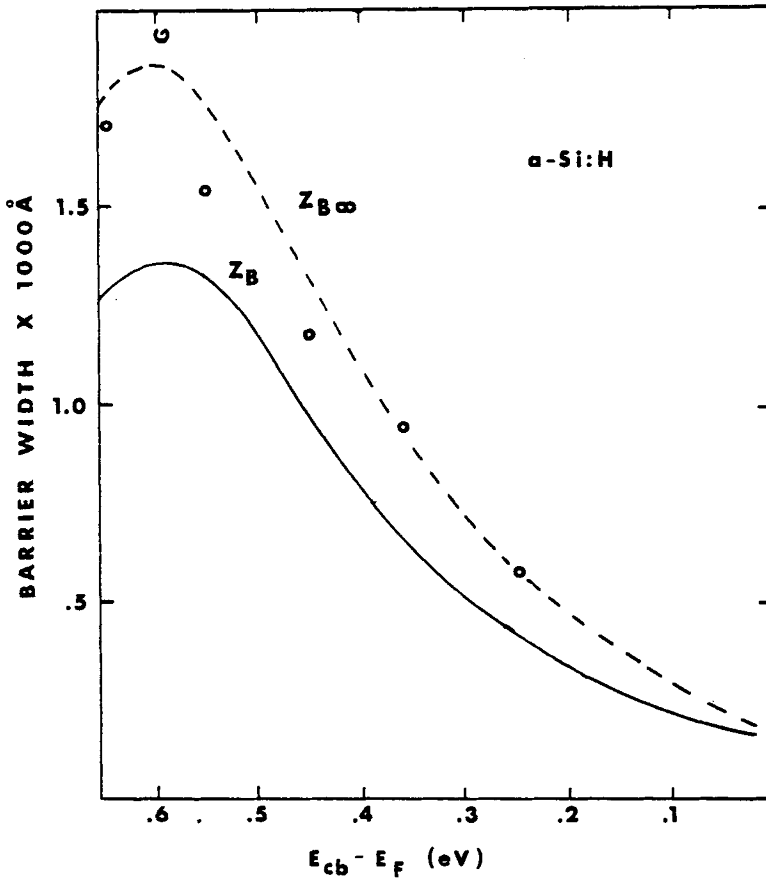

Fig. 11. The barrier width as a function of Fermi level for a-Si:H. The data points are taken from Ref. 13.

of states can be approximated by,

$$g = \frac{g_{min}}{2} \left[\exp - \frac{\varepsilon}{\varepsilon_{ch}} + \exp \frac{\varepsilon}{\varepsilon_{ch}} \right]$$

where ε is relative to the minimum density of states and ε_{ch} is a characteristic energy. For a-Si:H, $\varepsilon_{ch} \approx$ 0.094eV and for a-Si:F:H, $\varepsilon_{ch} = 0.066$eV. Fig. 10 shows the density of states which is assumed for the two types

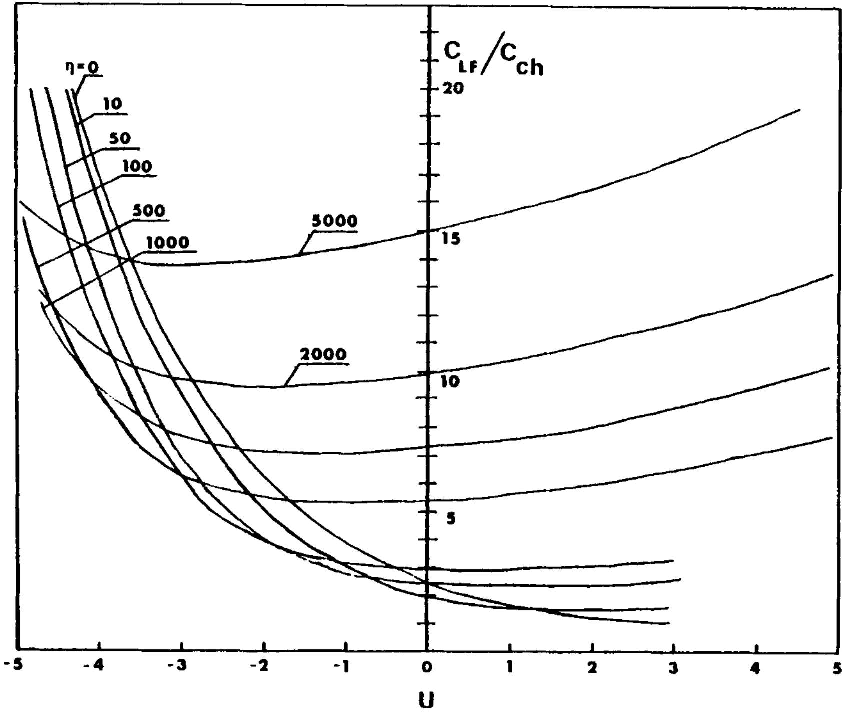

Fig. 12. Capacitance as a function of bias at low frequency. η refers to doping density. (12)

of alloys. The inset shows that a reasonable comparison exists between the assumed density of states and the measured density of states for a-Si:H. (6) The donor density is defined by,

$$g_n = \frac{g_{min}}{2} \exp\left(-\frac{\varepsilon}{\varepsilon_{ch}}\right)$$

and the acceptor density by,

$$g_p = \frac{g_{min}}{2} \exp\left(\frac{\varepsilon}{\varepsilon_{ch}}\right)$$

From this we can work out the space charge density as a function of the Fermi level position, which is controlled

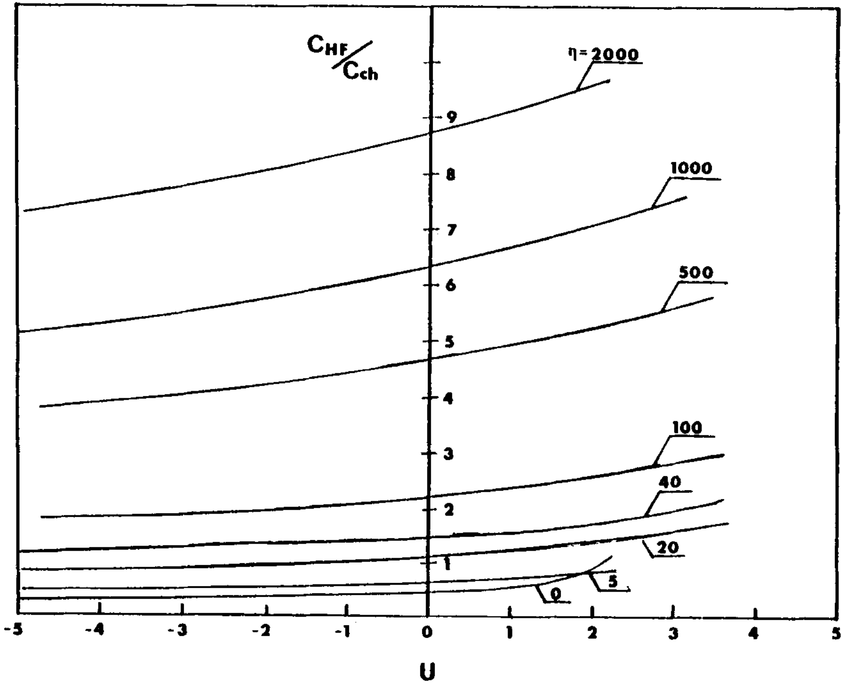

Fig. 13. Capacitance as a function of voltage at high frequencies. η refers to the doping density. (12)

by the doping. The shape and the width of the barrier can be analyzed by solving Poisson's equation. The solution to these equations can be described in a graphical form as shown in Fig. 11. In this Figure we show the width of the depletion layer as a function of the Fermi level position for a-Si:H and the points represent the results of the C-V interpretation of Spear et al. (13)

In the frame of this model, we show in Fig. 12 the low frequency capacitance (C_{LF}) as a function of forward and reverse bias for different doping densities η, where $\eta = N_D / \epsilon_{ch} g_{min}$, where $N_D cm^{-3}$ is the doping density and the dimensionless bias $U = qV/\epsilon_{ch}$, where V is the

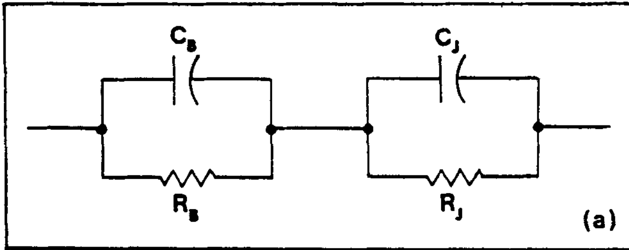

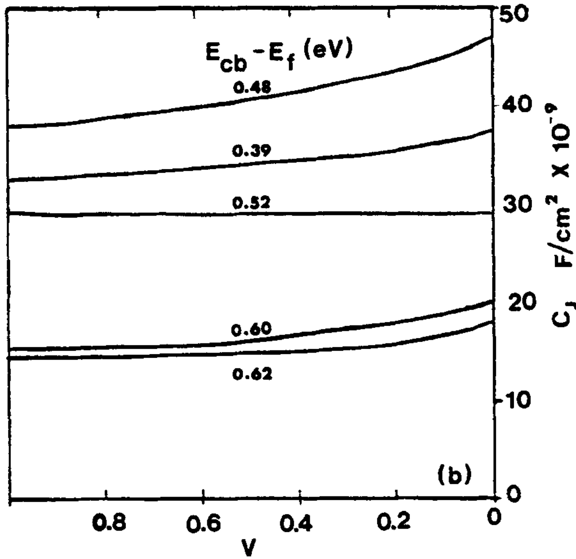

Fig. 14. (a) The equivalent circuit diagram as defined in the text.
(b) The variation of measured capacitance, C_J, as a function of reverse bias for samples with different activation energy, $(\varepsilon_C - \varepsilon_F)$, where ε_C is the conduction band and ε_F is the Fermi level. (12)

bias voltage. (12) C_{ch} is a characteristic capacitance and is proportional to $(g_{min})^{1/2}$. The change of shape at

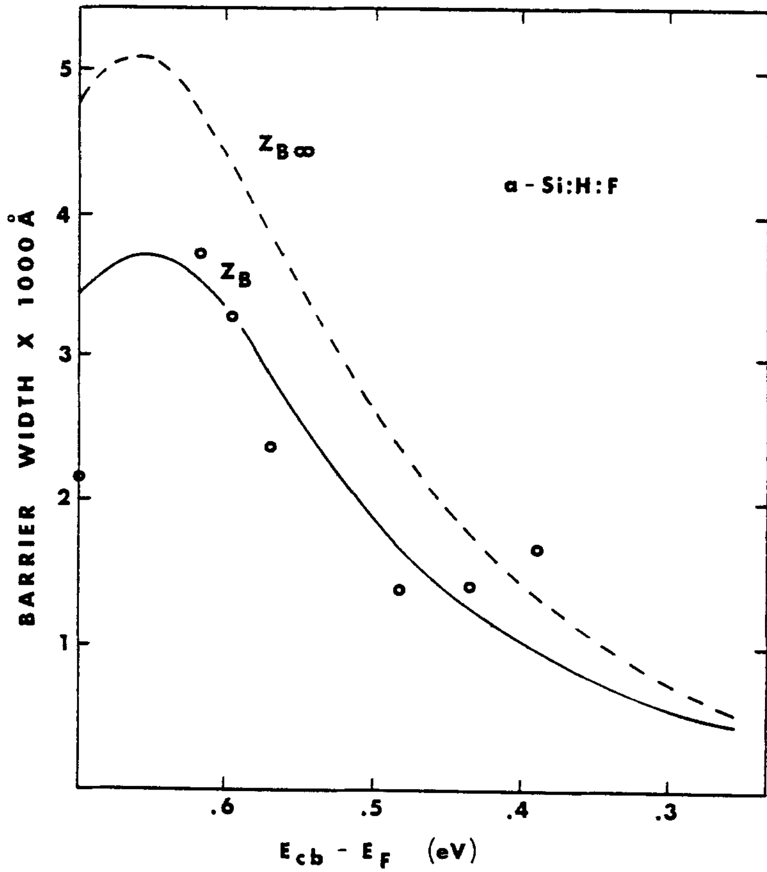

Fig. 15. The barrier width as a function of the Fermi level position for a-Si:H:F alloy. (12)

zero bias with increasing doping density is a characteristic behavior of amorphous materials and is directly attributable to deep localized states.

At high frequencies, the space charge does not respond to ac voltage variation. Thus, the depletion region behaves like a dielectric of thickness W_B sandwiched between two parallel plates. Therefore, the capacitance at

high frequency is simply

$$C_{HF} \propto \frac{1}{W_B}$$

where W_B is the barrier width. In the frame of this model, we can predict the C-V curves as a function of doping density n and is shown in Fig. 13 (12).

To test this we prepared devices in the following configuration. A thin n^+ layer ($\sigma_D > 10\ (\Omega\ cm)^{-1}$) was deposited on stainless steel substrate, followed by a 5000 Å thick active layer of a-Si:F:H with activation energy ranging from 0.71eV to 0.39eV. Finally, a thick Au layer was deposited to provide a Schottky barrier contact. The in-phase and out-of-phase components of these samples were measured and interpreted using the equivalent diagram shown in Fig. 14a. At high frequency, the dependence of the barrier capacitance C_J as a function of bias for different samples is shown in Fig. 14b. We should note that the general shape of the C-V is in quantitative agreement with the predictions of the model. This can now be reduced to the depletion width as function of the Fermi level position, as shown in Fig. 15. Our results suggest that the depletion width for a-Si:F:H is ~ 4000 Å , and for a-Si:H alloy, it is ~ 1500 Å .

Conclusion

We have shown above that an amorphous Si material containing F and H has a low density of states, possesses a high photoconductivity, can be easily doped, and possesses a wide depletion region.

In conclusion, we should mention that the photovoltaic devices fabricated from a-Si:H are often quoted to possess a depletion width of about 0.2μm (14) whicn is in good agreement with our results for a-Si:H. The inherently large density of states near the band edges leads to low values for the drift mobility and hence to low values for

the diffusion length of holes and electrons. Consequently, the predominant component of short-circuit current density is due to the drift within the depletion width rather than the diffusion of carriers. The drift current is related to the amount of effective absorption occurring within the depletion layer whose width in turn is limited by the density of states.

In the above, we have shown that in the a-Si:F:H, the depletion width is indeed widened. It is this aspect which provides for a potential for this material in photovoltaic devices.

Acknowledgements

We would like to thank L. Christian and R. Himmler for the preparation of samples and their assistance in measurements.

References

1. S.R. Ovshinsky, and A. Madan, in Proceedings of the 1978 Meeting of the American Section of the International Solar Energy Society, edited by Karl W. Böer and Alec F. Jenkins (AS of ISES, University of Delaware, 1978), p. 69.

2. S.R. Ovshinsky, and A. Madan, Nature 276, 482 (1978).

3. A. Madan, S.R. Ovshinsky, and E. Benn, Philos. Mag., in press.

4. A. Madan, and S.R. Ovshinsky, to be published in the Proceedings of the Symposium on Applied Technology to Solar Energy Systems, Jurica, Queretaro, Mexico, January 29 - February 3, 1979.

5. W.E. Spear, and P.G. Le Comber, J. Non-Cryst. Solids 8-10, 727 (1972).

6. A. Madan, P.G. Le Comber, and W.E. Spear, J. Non-Cryst. Solids 11, 219 (1976).

7. W.E. Spear, and P.G. Le Comber, Philos. Mag. 33, 935 (1976).

8. D.E. Carlson, and C.R. Wronski, J. Electron. Mater. 6, 95 (1977).

9. J.C. Knights, in Structure and Excitations of Amorphous Solids, edited by G. Lucovsky and F.L. Galeener (AIP, New York, 1976), p. 296.

10. N.F. Mott, and E.A. Davis, Electronic Properties in Noncrystalline materials (Clarendon Press, 1971).

11. N.F. Mott, Philos. Mag. 19, 835 (1969).

12. M. Shur, W. Czubatyj, and A. Madan, to be published.

13. W.E. Spear, P.G. Le Comber, and A.J. Snell, Philos. Mag., in press.

14. C.R. Wronski, D.E. Carlson, and R.E. Daniel, Appl. Phys. Lett. 29, 602 (1976).